Structural Performances of Thermoplastic Manufactured Parts

STEFAN TABACU[1], ANTON HADAR[2]*, DANUT MARINESCU[1], DUMITRU MARIN[2], GABRIELA DINU[2], DANIELA SMARANDA IONESCU[3]

[1]University of Pitesti, Mechanics and Technology, 1 Targu din Vale Str., 110040, Pitesti, Romania

[2]University Politehnica of Bucharest, IMST, 313 Splaiul Independentei, 060042, Bucharest, Romania

[3] Oradea University, Textiles and Leather, 1 Universitatii Str., 410087, Oradea, Romania

Thermoplastics are widely used for engineering application and customer goods. One of the application area is automotive industry. The passengers' compartment is an example of using high quality materials and advanced design solution in order to achieve aesthetic interiors and performance when safety is the issue. The impact of the passenger's head with the cockpit module is studied by experimental and numerical simulation. Material models are studied in order to obtain good results and to validate the numerical model for further investigation.

Keywords: thermoplastics, material characterization, impact, experiment, numerical simulation

Improving structural performances of thermoplastics manufactured parts represents a main objective of the researchers in various fields where these kind of parts are used.

Low specific weight and the application of complex geometry parts implied the use of thermoplastics as the main source material. It is the case of automotive industry where thermoplastics are used, as an example, for organising the passengers' compartment.

The acceptance of an automotive to be sold means that the product as an assembly must be validated under specific regulation. The most severe regulations are those regarding the passenger's safety in case of an impact. The passengers are protected using safety measures [1] and rational design of interior components.

In case when contact between the passenger and the interior of the vehicle occurs, the cinematic parameters record high variation within a very short time interval and, this determines high accelerations. The rules used for the model validation impose severe limits for these acceleration.

Biomechanical parameters that characterize the human body cannot be adapted to different impact situation so, the measure to be taken is to adapt the parts configuration and structural response to these parameters.

A validation process of the parts and components of the vehicle is initiated [2,3].

Experimental models used now are very sophisticated and can provide accurate information on the studied part.

One of the major shortcoming of experiments is that a new part is required for each run and the measurement chain must be constructed exactly the same way as the task book of the particular job assesses.

New methods for the investigation of structural performances are needed. The most used and important one is numerical simulation by the finite elements method [2-4].

Once the numerical model is validated using experimental data it may be used for detailed investigations of the structure. An optimization process is started and the best combination of materials and design rules is obtained.

There is also required an accurate information on the material being used and a numerical model that behaves according to the experimental test.

A significant number of injuries are due to the contact/ impact between the passenger's head and the cockpit module during a crash event [5]. Special safety requirements are stated for thermoplastics manufactured parts [6].

The interior components of the passengers' compartment must fulfill the requirements of ECE 21 (European Standard) [7] or FMVSS 201 (US Standard) [7].

Among these components the most complex is represented by cockpit module. It is also the most probable part to be impacted during a road event. The cockpit module consists in the instrument panel (fig. 1 – position 1), steering column, air conditioning (fig. 1 – position 2,3), glove box, cross car beam (fig. 1 – position 4), different storage area, navigation and audio system and different decorative elements.

The main components are made of polypropylene (PP) like ExxonMobil Chemical EXXTRAL® BMT 222 for the dashboard and ExxonMobil Chemical EXXTRAL® HMU 202 for the windshield demister.

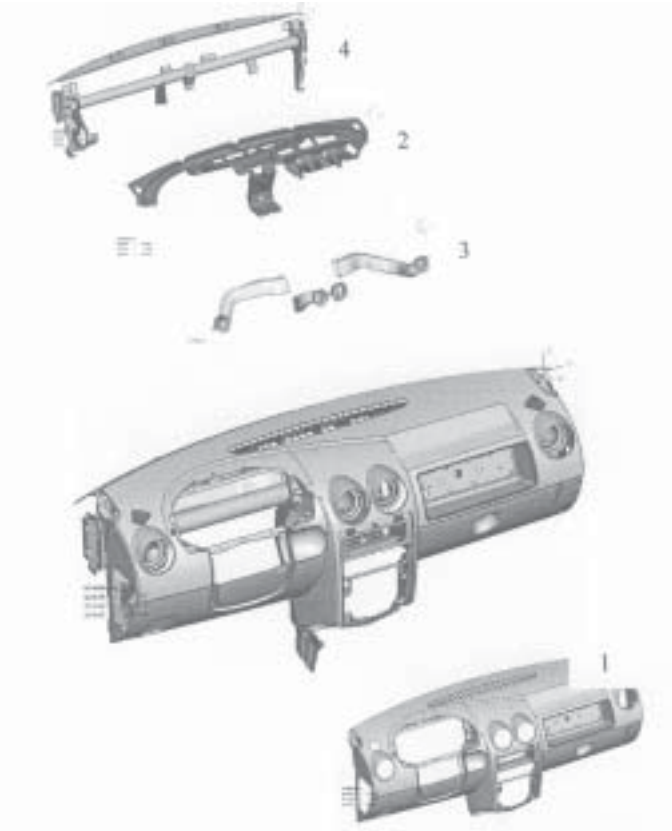

Fig. 1. Cockpit module

* *email: antonhadar@yahoo.com*

Mechanical characterisation of thermoplastics

For materials used in manufacturing the cockpit module the mechanical properties were obtained by performing a number of tensile experiments. A special test machine manufactured by Zwick/Roell was used. According to materials' specification datasheet, tensile testing velocity was 50 [mm/min].

Stress – strain curves σ - ε are the graphical representation of material's mechanical properties. These curves are plotted using the results from tensile experiments as tensile force versus specimen deformation. Figure 2 presents a specific tensile force versus specimen deformation curve for thermoplastic materials. In figure 2 there are represented a number of points like the elasticity limit (ΔLF_o, F_o), the maximum tensile force (ΔLF_n, F_n) and the tensile force in breaking (ΔLF_o, F_o) .

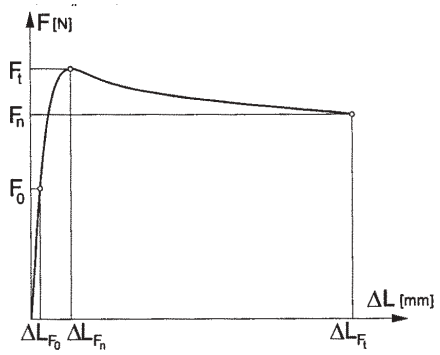

Fig. 2. Tensile force vs. specimen's elongation

Table 1 presents the value obtained for materials' physical and mechanical properties, according to manufacturer specification and tensile test results.

The differences between nominal and measured values could be explained by the fact that the specimen used in tensile test were considered from specific areas of the cockpit module, where the technological process may have altered mechanical properties.

In calculus there are used engineering stress equation (1):

$$\sigma_{nom} = \frac{F}{A_0} \tag{1}$$

and engineering strain equation (2):

$$\varepsilon_{nom} = \frac{L - L_0}{L_0} \tag{2}$$

where:

- F is the measured tensile force;
- A_o - the cross section area of the specimen;
- L is the specimen's length;
- L_o is the initial specimen's length;

So, the engineering stress – strain curve (fig. 3) is obtained.

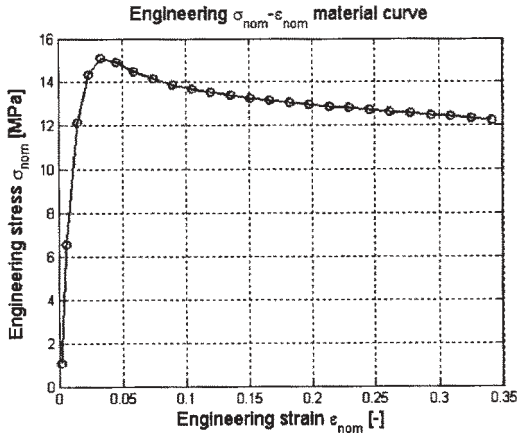

Fig. 3. Engineering stress - strain curve

For strain calculus, incremental method is used. The current stress – strain state of the specimen is a result of the anterior stress – strain state, thus the use of initial shape of the specimen to characterise the deformations may not be a good measure [9].

By incremental method, element strain is calculated with equation (3)

$$\varepsilon_{real\ i,j} = \frac{l_j - l_i}{l_i} \tag{3}$$

For the entire deformation process equation (3) becomes:

$$\varepsilon_{real} = \int_{L_o}^{L} \frac{l_j - l_i}{l_i} = \int_{L_o}^{L} \frac{dl}{l} = ln\frac{L}{L_0} \tag{4}$$

With equation (3) a correspondence between engineering and real strain can be set.

$$\varepsilon_{real} = ln\frac{L}{L_0} = ln\left(\frac{L_0 \cdot (1+\varepsilon_{nom})}{L_0}\right) = ln(1+\varepsilon_{nom}) \tag{5}$$

Table 1

MECHANICAL AND PHYSICAL PROPERTIES OF THE MATERIALS

Material name	Dimension	Nominal	Measured
ExxonMobilChemical **EXXTRAL BMT 222**	Density	$1040\ [kg/m^3]$	
	Elasticity modulus	$1800\ [MPa]$	$1250\ [MPa]$
	Maximum tensile force	-	$455\ [N]$
	Strain in necking	$3\ [\%]$	$3,5\ [\%]$
	Maximum stress	$18\ [MPa]$	$15,5\ [MPa]$
	Strain in breaking	$25\ [\%]$	$34\ [\%]$
	Specimen dimensions: Length $L_0 = 50\ mm$, Cross section area $A_0 = 30,1\ mm^2$		
ExxonMobilChemical **EXXTRAL HMU 202** (102942)	Density	$1040\ [kg/m^3]$	
	Elasticity modulus	$3250\ [MPa]$	$3050\ [MPa]$
	Maximum tensile force	-	$897\ [N]$
	Strain in necking	$4\ [\%]$	$4,5\ [\%]$
	Maximum stress	$32\ [MPa]$	$31,5\ [MPa]$
	Strain in breaking	$16\ [\%]$	$20\ [\%]$
	Specimen dimensions: Length $L_0 = 50\ mm$, Cross section area $A_0 = 28,5\ mm^2$		

For a complete material characterization, the specimen change of shape in tensile must be considered. Thus the traction force when necking occur must be identified. The engineering stress – strain curve is used. The necking point yields a value for $\frac{\partial \sigma_{nom}}{\partial \varepsilon_{nom}}$ gradiend of zero. This point also is considered to be the limit of deformation elastic domain. Elastic deformations appear because of hydrostatic stress and are characterized by an increase of the specimen's volume while accumulating strain energy. In the plastic domain of deformations, shear stresses are present and material flow takes place in a constant volume.

An element volume V with a cross section area A and not-deformed length l^d is further considered.

While deformations are in the elastic domain the element volume is $V_{neck} = A_{nneck} \cdot l^d_{neck}$ and the current cross section area is A_{neck} equal to the initial value A_o and $l^d_{neck} = l^d \cdot (1 + \varepsilon_{neck})$. Once necking occur, material flows in constant volume dV = 0.

Thus:

$$1 = \frac{V_n}{V} = \frac{A_0 \cdot l^d_n}{A \cdot l^d} = \frac{A_0}{A} \cdot \frac{l_0}{l_0} \cdot \frac{1 + \varepsilon_n}{1 + \varepsilon} \quad (6)$$

where V is the current volume, A is the current cross section area and l^d is the current element's length.

Using equation (7)

$$\frac{\sigma_n}{\sigma} = \frac{\frac{F_n}{A_o}}{\frac{F}{A}} = \frac{F_n}{F} \cdot \frac{A}{A_o} \quad (7)$$

it can be obtained (equation (8)):

$$\sigma_{real} \equiv \sigma = \sigma_n \cdot \frac{A_0}{A} \cdot \frac{F}{F_n} = \frac{F_n}{A_0} \cdot \frac{F}{F_n} \cdot \frac{1 + \varepsilon}{1 + \varepsilon_n} = \frac{F}{A_0} \cdot \frac{1 + \varepsilon}{1 + \varepsilon_n} \quad (8)$$

or (equation (9))

$$\sigma_{real} = \frac{F}{A_0} \cdot \frac{1 + \varepsilon}{1 + \varepsilon_n} \quad (9)$$

so, a relation between engineering and real stress is defined. Engineering current strain ε and engineering strain at necking ε_n are both used in equation (9).

It is worth mentioning the fact that for thermoplastics necking occurs at higher strain 3 ÷ 5% compared to metals where yielding occurs at lower strain 0.1 ÷ 0.2%.

Commonly used equation (10) for the definition of real stress does not consider the necking point as the ultimate coordinate before the cross section of the specimen would change, thus a higher value for the real stress is obtained [10].

$$\sigma_{real} = \sigma_{nom} \cdot (1 + \varepsilon_{nom}) \quad (10)$$

Figure 4 presents the materials curves both in engineering stress – strain and real stress strain coordinates.

For the validation of the material model (equation (9), equation (10)) numerical simulation by finite elements method was used. The numerical models were solved using LS-Dyna v.970 code, an explicit, general purpose, widely appreciated solver for transient, slow and high velocity dynamics simulations [10,11].

Figure 5 presents the specimen's shape change while tensile and also the section where necking occurs.

The calculation of tensile force is performed and results are compared to the ones from experiments. Figure 6a presents the tensile force, calculated tensile force for a material formulation when the real stress – strain curve

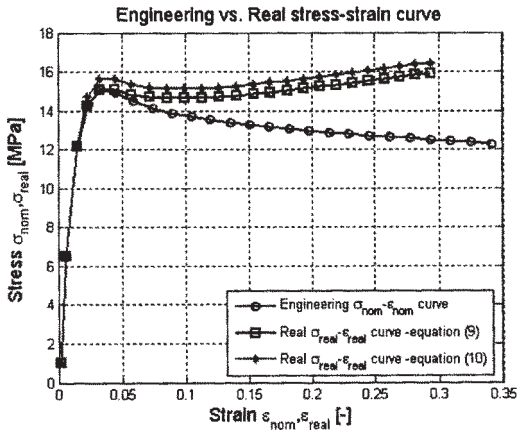

Fig. 4. Engineering real stress - strain curves

Fig. 5. Numerical simulation of specimen's traction test

was created using equation (9) and the calculated tensile force for a material formulation when the real stress – strain curve was created with equation (10).

For a better appreciation of the material mathematical models figure 6b presents the error obtained between the nominal tensile force and calculated ones.

An evaluation of the error in the measured and calculated tensile force pointed that equation (9) offered a better definition of the real stress – strain curve.

Figure 7 presents the real stress – strain curves for all thermoplastic materials used in manufacturing the cockpit module.

Evaluation of the part structural performances

Once the mechanical and physical properties of the materials were defined the numerical model may be validated.

Experiments were performed and the structural performances of an existing cockpit module evaluated. For EU countries experiments are performed according to ECE 21 specifications using a gravitational pendulum consisting in a spherical rigid impactor that is supported by a rigid frame with roll bearings [12].

The impact area was determined by numerical simulation (fig. 8), thus the impact area between the passenger's head and the cockpit module was defined [1,14].

Special transducers were used to measure the impact parameters, like the impactor acceleration during the event, structure response (acceleration) and impactor arm angular velocity. Figure 9 presents the test rig and the data acquisition solution used in experiments.

The numerical model was built using more than 120.000 shell finite elements with less than 5% of then being triangles. The main components of the cockpit module were defined as different *parts* [11] according to the properties of material type and thickness.

The main elements were linked together using rigid constrains (*CONSTRAINED_NODAL_RIGID_BODY) or

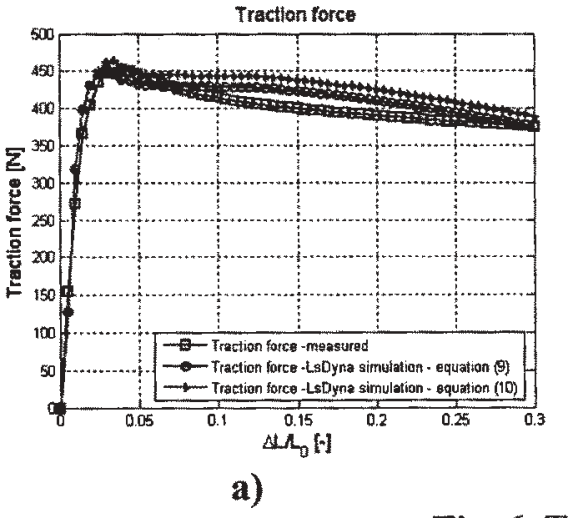

a)

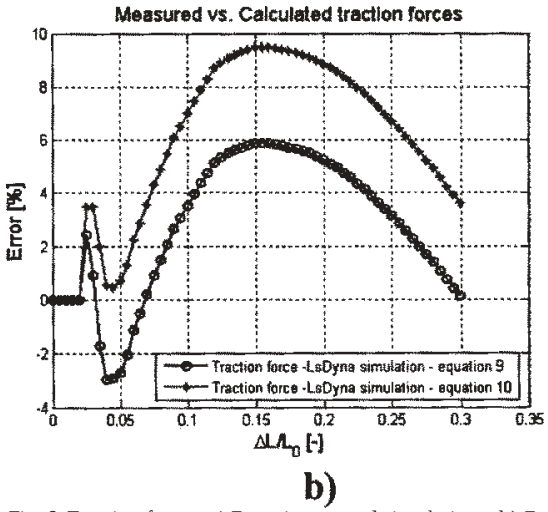

b)

Fig. 6. Traction force. a* Experiment and simulations, b) Error

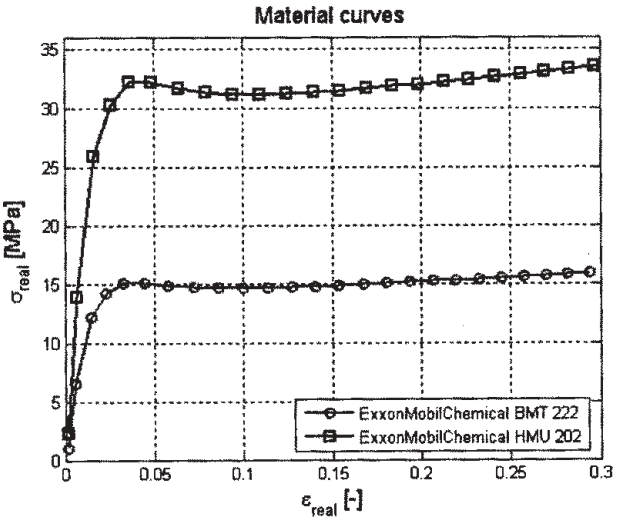

Fig. 7. Materials real stress / strain curves

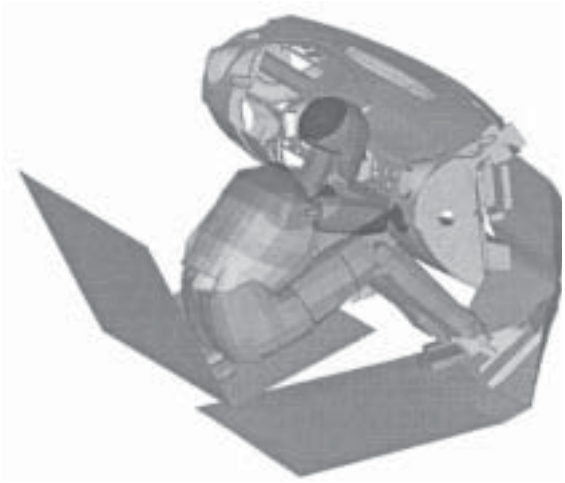

Fig.8. Passengers impact with the cockpit module

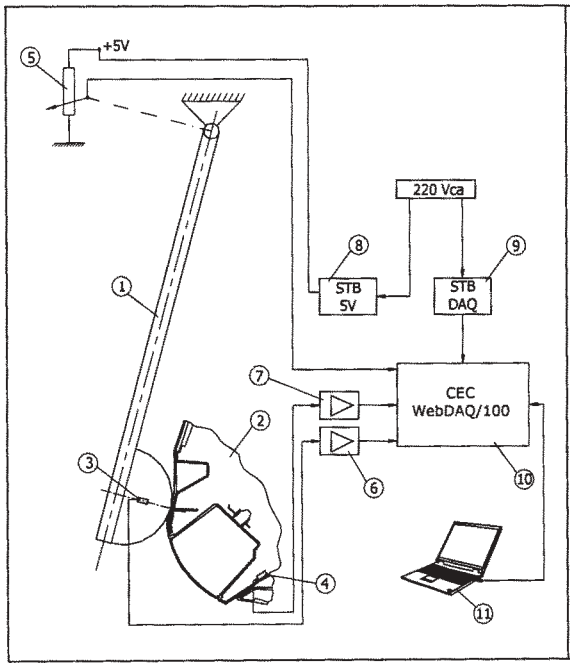

Legend:

1 – Pedulum;
2 – Cockpit module;
3 – ***MMF KB 10 3081*** accelerometer mounted inside the impactor;
4 – ***PCB Piezotronics 333B42*** accelerometer mounted on the dashboard;
5 – transducer for the measurement of the arm's angular velocity;
6 – ***RFT 11015*** signal amplifier mounted inside the impactor;
7 – ***PCB Piezotronics 480E09*** signal amplifier of the accelerometer mounted on the dashboard;
8 – stabilised power source of the transducer for the angular velocity;
9 – stabilised power source for the data acquisition system;
10 – ***CEC WebDAQ/100*** –data acquisition system;
11 – *laptop* runnning Win XP OS and *software* for the data acquisition system.

Fig.9.Data acquisition solution for experimental testing

elastic (*ELEMENT_DISCRETE) ones. The structure was constrained in motion and support defined (*BOUNDARY_SPC). As there are many parts in the model a method for interference between them was required thus contact was added (*CONTACT_ AUTOMATIC_ SURFACE_ TO_SURFACE). For parts in contact with different stiffness, a contact parameter was defined and used (SOFT). Also, thickness and contact forces were analysed in order to evaluate them influence over the simulation results. Mass compensation was used for the other components that were not represented in the cockpit module model.

The structure's response, while the impact depends on the material characteristics used. In order to do it, there was defined a typical material card. (MAT24

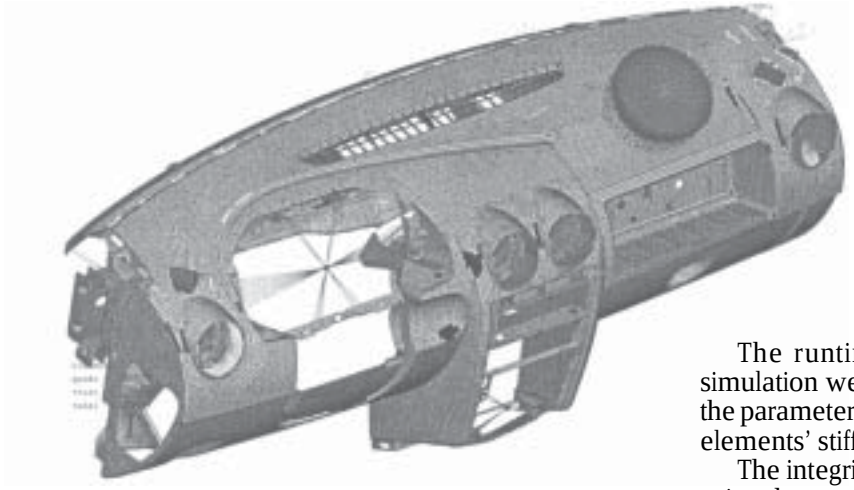

Fig. 10. The numerical model

*MAT_PIECEWISE_LINEAR_PLASTICITY).

The reduced mass of the impactor used for the numerical simulation is of 6.8 kg. Its initial velocity is of 24.1 [km / h] when an area that does not contain airbag systems is impacted and it is reduced to 19.3 [km / h] for that particular cases.

The impactor is perfectly rigid (MAT20 *MAT_RIGID). The units system used for simulation are defined by mm for lengths, *ms* for time, kg / mm^3 for density, and thus, resulted kN for forces and *J* for energy.

The numerical model is presented in figure 10.

The head trauma is evaluated using a special parameter named HIC (Head Injury Criteria) defined by equation (11). The criterion is calculated while an interval of 36 miliseconds or 15 miliseconds, The value must not exceed 1000 units.

$$HIC = \left[\frac{1}{t_2 - t_1} \cdot \int_{t_1}^{t_2} \frac{a}{g} \cdot dt \right]^{2.5} \cdot (t_2 - t_1) \qquad (11)$$

where *a* is the measured acceleration, *g* is the gravitational acceleration.

Results and discussion

The data obtained in experiments were checked for integrity. Using calibration devices, the measured data were transformed into the units system used in this study. The impactor's velocity was the one required by the standard (ECE 21). Once this validation was performed the data from the impactor's accelerometer were post-processed. The sample rate used for recording the signal was of 5000 Hz and a post-treatment of the signal was performed using Wavemenu Toolbox available in MATLAB [15].

The numerical simulation was performed using PC machines with Intel®Core2Duo™ at 2.4 GHz CPU and 2 Gb of RAM and Intel®Core2Quad™ at 2.4 GHz CPU and 4 Gb of RAM.

The runtime was about 1 h and a number of 20 simulation were performed with a wide variation field of the parameters defined in the model construction (contact, elements' stiffness, constrains)

The integrity of the numerical model was checked out using the energy balance. The total system energy had to be equal to the sum of the kinetic energy of the impactor and the internal energy accumulated by the elements of the cockpit module.

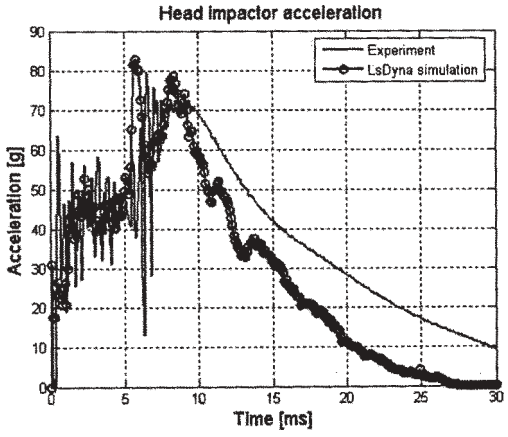

Fig..11. Impactors CG acceleration

The event duration is of 30 ms and the peak acceleration was recorded within the first 10 miliseconds.

Figure 11 presents the accelerations obtained after the experiment and simulation were performed according to ECE 21 specifications.

It may be noticed a good correlation of the data obtained in experiment with the ones obtained by simulation.

The acceleration curve presents two peaks. The first peak is at 5 ms and an acceleration of 50 g is recorded, while the second peak is at 9 ms and an acceleration of 80 g, as the maximum values, is stated. The event period is less than 36 miliseconds thus HIC was calculated during a 15 miliseconds time interval. For the numerical simulation HIC_{15ms} = 259.9 was obtained, while for experiment it was HIC_{15ms} = 248.8, implying an error of measured and

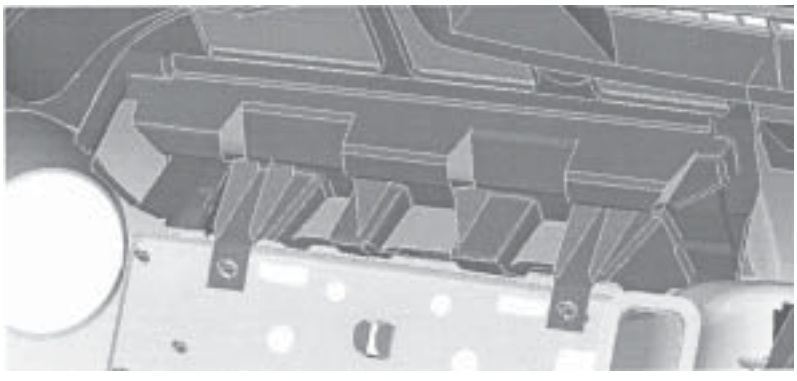

Fig..12. The initial configuration of the structure

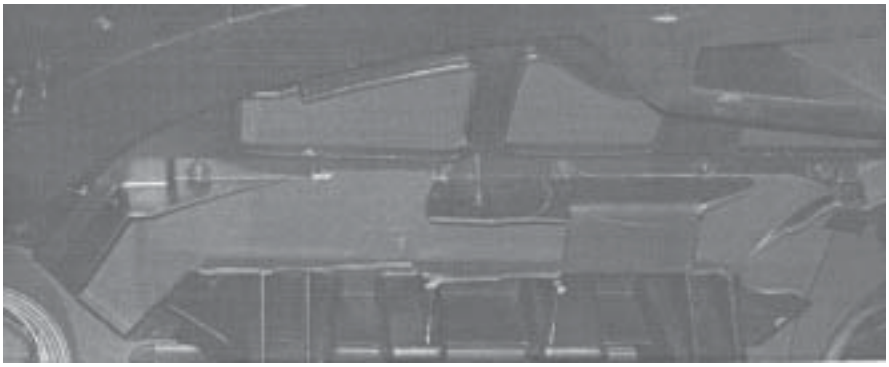

Fig.13. Damaged structure - experiment

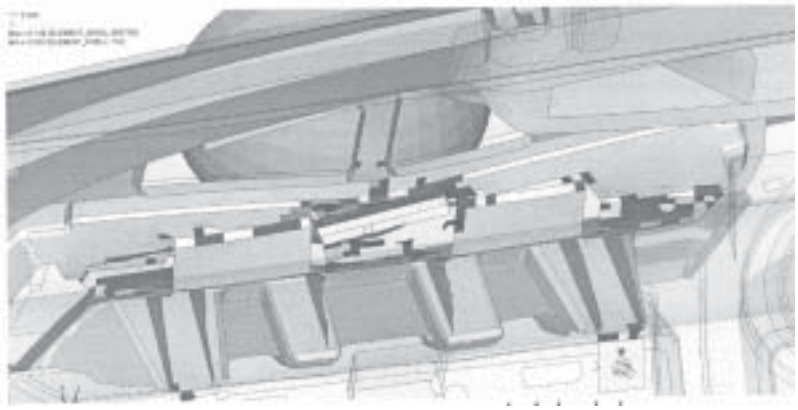

Fig.14. Damaged structure - numerical simulation

calculated data about 4.25%. The parameters are within the limits of ECE 21 specifications.

Using the numerical model, the deformation energy consumed by each individual component may be evaluated. Thus the component with the main contribution is identified and an optimization process may de initiated [16]. Figure 12 presents the initial configuration of the structure. Figure 13 presents the damaged structure after performing the experiment while figure 14 presents the damaged structure after performing the numerical simulation.

One can notice the good agreement between the damage pattern obtained after experiments and the one obtained after numerical simulation. The differences that exist are due to manufacturing process – weld lines and air traps, and differences between the nominal and real thicknesses of the parts.

Conclusions

Once the numerical model validated for impact situation, it may be further used for the process optimization, which can be performed using only numerical simulation; thus the development process and costs decrease. If experimental testing requires a new part to be tested every time it is performed, when a virtual prototype is available the number of changes is unlimited and the best solution may be faster identified and used for the design and manufacturing process.

Further research will evaluate the performances of polymer cellular materials (foams) [17,18] or composite materials [19,20] in order to improve the impact response and to increase the passengers' safety in case of an road event.

References

1. MA,D., ZHANG, H., Int. J. Crashworthiness **11**, 2006, p.243
2. LUPEA, I., CORMIER, J., Mat. Plastice, **44**, nr. 4, 2007, p.339
3. FREMGEN, C., MKRTCHYAN, L., HUBER, U., MAIER, M., Sci. Techol. Advanced Mater. **6**, 2005, p.883
4. DAVOODI, M.M., SAPUAN, S.M., YUNUS, R., J. Mater. Design, 2007, article in press
5. FMVSS: Head Impact Protection, National Highway Traffic Safety Administration (NHTSA), http:/www.nhtsa.gov/cars/rules/rulings/headprot/pubnprm.html
6. DEB, A., GUPTA, N.K., BISWAS, U., MAHENDRAKUMAR, M.S., Int. J. Crashworthiness, **10**, 2005, p.249
7. *** htpp://www.crash-network/regulations
8. YEO, T.J, PARK, J., A unified FE modeling approach to an automobile cockpit module, 2003 ABAQUS Users' Conference.
9. ROWE, G.W., STURGES, C.E.N., HARTLEY, P., PILLINGER, I., Finite element plasticity and metalforming analysis, Cambridge University Press, 1991, 2005 edition, ISBN 13 978-0-521-31731-2, p.40-48, 66-79
10.DU BOIS, P., 'Crashworthiness Engineering. Course Notes', Livermore Software technology Corporation, 2004.
11. Livermore Software Technology Corporation, 'LS-DYNA Keyword Manual v970', Livermore, CA, Livermore Software Technology Corporation, April 2003
12. ILIE, S., TABACU, ªt., TABACU, I., NICOLE, V., ªERBAN, F., Acta Technica Napocensis, Series Applied Mathematics and Mechanics **50**, V, 2007, p.149
13. TABACU, ªT., ILIE, S., NICOLAE, V., IVÃNESCU, M., STÃNESCU, N.D., Acta Technica Napocensis, Series Applied Mathematics and Mechanics **50**, V, 2007, p.187
14. DEB, A., TAHSIN, A, Int. J. Impact Eng. **30**, 2004, p.521
15. The Mathworks Inc., 'MATLAB Users Guide (R14)', The Mathworks Inc
16. FANG, H., RAIS-ROHANI, M., LIU, Z., HORSTMEYER, M.F., Computer Struct. **83**, 2005, p.2121
17.Du BOIS, P.A., KOLLING, S., KOESTERS, M., FRANK, T., Int. J. Impact Eng. **32**, 2006, p.725
18.RIZZI, E., PAPA, E., CORIGLIANO, A., Int. J. Solids and Struct., **27**, 2000, p.5773
19.HADĂR, A., CONSTANTINESCU, I.I., JIGA, G., IONESCU, D.S., Mat. Plastice, **44**, nr. 4, 2007, p.354
20. CHUNG, J.G., CHANG, S.H., SUTCLIFFE, M.P.F, Compos. Sci. Technol. **67**, 2007, p.2342

Manuscript received: 10.12.2007